

UNCLASSIFIED

Defense Technical Information Center
Compilation Part Notice

ADP014114

TITLE: Development of Discontinuous Galerkin Method for the Linearized Euler Equations

DISTRIBUTION: Approved for public release, distribution unlimited
Availability: Hard copy only.

This paper is part of the following report:

TITLE: Aging Mechanisms and Control. Symposium Part A -
Developments in Computational Aero- and Hydro-Acoustics. Symposium
Part B - Monitoring and Management of Gas Turbine Fleets for Extended
Life and Reduced Costs [Les mecanismes vieillissants et le controle]
[Symposium Partie A - Developpements dans le domaine de
l'aeroacoustique et l'hydroacoustique numeriques] [Symposium Partie B ...

To order the complete compilation report, use: ADA415749

The component part is provided here to allow users access to individually authored sections of proceedings, annals, symposia, etc. However, the component should be considered within the context of the overall compilation report and not as a stand-alone technical report.

The following component part numbers comprise the compilation report:

ADP014092 thru ADP014141

UNCLASSIFIED

Development of Discontinuous Galerkin method for the Linearized Euler equations

Carl Blom,

Phd. student, Department of Mechanical Engineering, University of Twente,
P.O. Box 217, 7500 AE, Enschede, The Netherlands, c.p.a.blom@wb.utwente.nl

Rob Hagmeijer,

Associate Professor, Department of Mechanical Engineering, University of Twente,
P.O. Box 217, 7500 AE, Enschede, The Netherlands, r.hagmeijer@wb.utwente.nl

Eric Védý,

Phd, Acoustics Division, TNO Institute of Applied Physics,
P.O. Box 155, 2600 AD, Delft, The Netherlands, vedy@tpd.tno.nl

1 Introduction

The propagation of sound waves, defined as an oscillatory motion with small amplitude in a compressible fluid [1], can be described by the linearized Euler equations (LEE), under the assumptions that there is no feedback to the mean-flow and that effects of viscosity and heat conduction can be neglected.

In the field of Computational Aeroacoustics (CAA), it is widely recognized that the numerical algorithms applied to solve the governing equations must have sufficiently low numerical dispersion and dissipation in order to accurately simulate the propagation of aeroacoustic information. To this end, higher-order schemes can be used. The Discontinuous Galerkin (DG) [2, 3] method is an ultimately compact finite-element method which can be applied efficiently on unstructured meshes, thus allowing geometrically complex problems to be handled. Higher-order (higher than second-order) accuracy can be obtained relatively easily because of the compactness of the method, at the penalty, however, of an increasing number of unknowns per element. An extensive description of the application of the Discontinuous Galerkin method in the field of CAA is given by Atkins *et al.* [4, 5, 6, 7].

The results presented in the present paper are obtained with the computer code DIGS3D, which is based on a numerical algorithm developed to solve the LEE in three dimensions. For the spatial discretization of the LEE the Quadrature-free Discontinuous Galerkin method has been applied, while the time integration is performed by a four-step, low-storage Runge-Kutta algorithm. At present the algorithm is second-order accurate in both space and time. The numerical algorithm has already been applied to a three-dimensional broadband cavity-noise prediction problem [8], where it is part of a three-step method. In the three-step method, the first step provides the time-averaged RANS-solution from which, in the second step, turbulent aeroacoustic source terms for the LEE are obtained. In the third step DIGS3D is used to simulate the propagation of the aeroacoustic disturbances produced by the source field.

The work presented in this paper can be regarded as a continuation of the work presented in [9]. In [9] two verification problems, the convection of a 2D compact acoustic disturbance and the radiation from a three-dimensional harmonic monopole source, were presented. One of the conclusions drawn in that paper is that acceleration of the algorithm to relax requirements on computational effort was needed. Here we present results obtained for the first of the two

Research has been carried out within the UT-TNO Sound & Vibrations Research Centre

aforementioned verification problems, obtained with a parallelized version of the code. The algorithm is parallelized employing MPI (Message Passing Interface) and the code is run on a 1024-CPU platform (TERAS [10]). A more thorough description of parallelizing a DG-based CAA-algorithm, employing MPI, is presented in [11]. The main objectives of the work presented in the present paper are (continuation of) the verification of the numerical algorithm and conducting a performance test of the parallelized algorithm on TERAS.

The outline of the paper is as follows: In the first section the governing equations, i.e. the Linearized Euler equations (LEE), are presented. In the second section the Quadrature-free Discontinuous Galerkin method is briefly described. The next section describes the convection of a two-dimensional compact acoustic disturbance in a uniform mean flow. The analytical solution of the problem is presented and the obtained numerical results are compared with the analytical solution. Furthermore results of a performance test on TERAS are presented. Subsequently, concluding remarks and suggestions for further research are given.

2 Linearized Euler Equations

Consider the dimensionless linearized Euler equations (LEE) in conservation form in three spatial dimensions

$$\mathbf{L}(\mathbf{U}) \equiv \frac{\partial}{\partial t} \mathbf{U} + \frac{\partial}{\partial x_j} \mathbf{F}_j(\mathbf{U}) = \mathbf{S}, \quad \mathbf{U}(\mathbf{x}, t), \quad (\mathbf{x}, t) \in \Omega \times (0, T), \quad (1)$$

where

$$\mathbf{F}_j(\mathbf{U}) = \mathbf{A}_j(\mathbf{U}_0)\mathbf{U}, \quad \mathbf{A}_j \in \mathbf{R}^5 \times \mathbf{R}^5, \quad (2)$$

with initial and boundary conditions. Here $\mathbf{S} \in \mathbf{R}^5$ is the source term for the LEE, $\Omega \in \mathbf{R}^3$ is an open domain with boundary $\partial\Omega$ and $t \in (0, T)$ denotes time. The summation convention is used on the repeated index j , where $j = 1, 2, 3$. $\mathbf{U} = (\rho', u'_1, u'_2, u'_3, p')^T$, where the components of the vector denote the dimensionless aeroacoustic density perturbation, the three velocity perturbation components and the pressure perturbation, respectively. The components of vector \mathbf{U}_0 denote the dimensionless quantities related to the mean flow density, the three components of the mean flow velocity and the mean flow pressure. The matrices \mathbf{A}_j are defined as:

$$\mathbf{A}_j(\mathbf{U}_0) = \begin{bmatrix} M_j & \delta_{j1} & \delta_{j2} & \delta_{j3} & 0 \\ 0 & M_j & 0 & 0 & \delta_{1j} \\ 0 & 0 & M_j & 0 & \delta_{2j} \\ 0 & 0 & 0 & M_j & \delta_{3j} \\ 0 & \delta_{j1} & \delta_{j2} & \delta_{j3} & M_j \end{bmatrix}, \quad (3)$$

where M_1, M_2, M_3 are the components of the mean flow Mach-number in x, y and z-direction, respectively, and δ_{ij} denotes the Kronecker-delta symbol.

3 Quadrature-free Discontinuous Galerkin Method

In this section we briefly describe the Quadrature-free Discontinuous Galerkin spatial discretization. In [8] a more detailed description is presented. Throughout this section we have $i \in [1, N_e]$,

$k \in [0, M]$ and $l \in [0, M]$.

Let us define the solution space V defined on Ω , let $\mathbf{U} \in V$ and let the inner product on V be defined as:

$$\langle u, v \rangle \equiv \int_{\Omega} u(\mathbf{x})v(\mathbf{x})d\mathbf{x}, \quad (4)$$

from which we can define [12] the L^2 -norm $\|u\| = \sqrt{\langle u, u \rangle}$.

The domain Ω is partitioned into non-overlapping elements Ω_i , $\Omega = \cup \Omega_i$. Let $V_h \subset V$ be a finite-dimensional subspace, spanned by the linearly independent basis functions b_{ik} , and let $\mathbf{U}_h \in V_h$. \mathbf{U}_h is obtained by the projection of \mathbf{U} onto the subspace $V_h = \text{span}\{b_{ik}\}$:

$$\mathbf{U}_h = \sum_{i=1}^{N_e} \sum_{k=0}^M \mathbf{v}_{ik}(t)b_{ik}(\mathbf{x}). \quad (5)$$

In the Discontinuous Galerkin formulation the unknown coefficients \mathbf{v}_{ik} are obtained by solving the system of equations given by:

$$\langle \mathbf{L}(\mathbf{U}_h), b_{il} \rangle = \langle \mathbf{S}, b_{il} \rangle, \quad \forall (i, l). \quad (6)$$

Partial integration of Eq.(6) yields:

$$\langle b_{il}, b_{ik} \rangle \frac{d\mathbf{v}_{ik}}{dt} - \left\langle \frac{\partial b_{il}}{\partial x_j}, \mathbf{A}_j b_{ik} \right\rangle \mathbf{v}_{ik} + \int_{\Gamma_i} b_{il} b_{ik} (\mathbf{A}_j \mathbf{n}_j) \mathbf{v}_{ik} d\Gamma = \langle b_{il}, \mathbf{S} \rangle, \quad \forall (i, k, l), \quad (7)$$

where $\Gamma_i = \partial\Omega_i$ and \mathbf{n} is the unit outward normal to boundary Γ_i .

Closer inspection of both Eq.(6) and Eq.(7) reveals that the solution within an element only depends on information within that element, i.e. there is no "communication" between elements. Furthermore the global solution is, in general, discontinuous over an element interface. To provide the crucial coupling and to handle the discontinuity at element interfaces, the boundary-normal flux, $\mathbf{F}_j(\mathbf{U}_h)\mathbf{n}_j = \mathbf{A}_j \mathbf{n}_j \mathbf{U}_h$, is modeled by means of an approximate Riemann flux $\mathbf{F}_j^R(\mathbf{U}_L, \mathbf{U}_R)\mathbf{n}_j$, where \mathbf{U}_L and \mathbf{U}_R represent \mathbf{U}_h on either side of the element interface. For the present implementation of the method we approximate the Riemann flux by the Lax-Friedrichs flux, which can be written as:

$$\mathbf{F}_j^R(\mathbf{U}_L, \mathbf{U}_R)\mathbf{n}_j = \frac{1}{2} \{ [\mathbf{F}_j(\mathbf{U}_L) + \mathbf{F}_j(\mathbf{U}_R)]\mathbf{n}_j - \alpha(\mathbf{U}_R - \mathbf{U}_L) \}, \quad (8)$$

where \mathbf{n} points from element L to element R and α is a positive quantity that is larger in magnitude than the eigenvalues of the Jacobian of $\frac{1}{2}[\mathbf{F}_j(\mathbf{U}_L) + \mathbf{F}_j(\mathbf{U}_R)]\mathbf{n}_j$.

For a quadrature-free implementation [4] of Eq.(7) the source-term in the LEE (also) has to be projected onto V_h :

$$\mathbf{S}_h = \sum_{i=1}^{N_e} \sum_{k=0}^M \mathbf{s}_{ik}(t)b_{ik}(\mathbf{x}). \quad (9)$$

Since the LEE are linear, $\mathbf{F}_j(\mathbf{U}_h)$ is expanded in a natural way as can be seen from Eq.(7). Furthermore, Atkins and Lockard [5] report that for the simulation of the scattering of acoustic waves (where an assumption of linearity can be made) it is sufficient to represent the mean flow by a lower-order polynomial to ensure the formal order properties of the method.

Johnson and Pitkäranta [2] prove that when the basis functions are polynomials of degree p , the order of accuracy is at least $p + \frac{1}{2}$. In most practical cases [4] the order of accuracy is observed

to be $p + 1$. With the relation between M , p and the number of space-time dimension d given by [4]:

$$M(p, d) = -1 + \frac{1}{d!} \prod_{k=1}^d (p + k), \quad (10)$$

this implies that in order to obtain second-order accuracy we must choose $p = 1$, resulting in $M = 3$ for $d = 3$.

Eq.(7) is conveniently evaluated through the introduction of computational coordinates. These coordinates are local to a reference element for which we choose an equal-sided tetrahedron. Within the reference element we define the basis set, consisting of monomials, as $b_k \in \{1, \xi, \eta, \zeta\}$. The time integration is performed by a second-order accurate, four-step, low-storage Runge-Kutta algorithm [13].

The Discontinuous Galerkin method, due to its local character, is very well suited for parallel calculations. The present parallel implementation is based on a domain decomposition of the unstructured mesh into several blocks where the calculation for each block is performed on a different processor. The MPI (Message Passing Interface) routines are used to communicate data between processors for the flux calculations at the interfaces of elements belonging to different partitions. The block partitioning itself, is based on the METIS ([14]) libraries, and is optimized in order to achieve both a quasi-uniform loading on the processors, and to lower the communication costs during computation (minimization of the number of interfaces).

4 Convection of a 2D Compact Acoustic Disturbance

4.1 Problem description

In this verification case the LEE (Eqs.(1) to (3)) are solved on a square domain in which a compact acoustic perturbation is imposed through the initial conditions. The two-dimensional domain has dimensions $x \in [-100, 100]$, $y \in [-100, 100]$ and the acoustic source is initially centered at $x = y = 0$. The mean flow is uniform with Mach-number components $M_1 = M = 0.5$ and $M_2 = 0$, there are no sources ($\mathbf{S} = \mathbf{0}$) and the initial condition for the 2D solution vector $\mathbf{U}(x, y, t) = (\rho', u', v', p')^T$ is given by:

$$\mathbf{U}(x, y, 0) = \begin{pmatrix} f(x, y) \\ \beta x f(x, y) \\ \beta y f(x, y) \\ f(x, y) \end{pmatrix}, \quad (11)$$

with

$$f(x, y) = e^{-\alpha(x^2+y^2)}, \quad \alpha = \frac{\ln(2)}{9}, \quad \beta = 0.04. \quad (12)$$

This test case has also been addressed by Atkins and Shu [4]. Together with a vorticity wave it is furthermore described as part of the ICASE/LARC Workshop on Benchmark Problems in Computational Aeroacoustics [15]. Note, however, that in the benchmark-case the initial velocities, u' and v' , are taken equal to zero.

4.2 Analytical solution

The LEE, together with the conditions described above, can be transformed into the wave equation:

$$\frac{D^2 q}{Dt^2} - \nabla^2 q = 0, \quad \text{with} \quad \frac{D}{Dt} = \frac{\partial}{\partial t} + M \frac{\partial}{\partial x}, \quad (13)$$

where q is either one of the primitive variables ρ' , u' , v' or p' .

Upon introducing a coordinate system moving with the mean flow: $\tau = t$, $\xi = x - Mt$, $\eta = y$, the wave equation can be written as:

$$\frac{\partial^2 q}{\partial \tau^2} - \tilde{\nabla}^2 q = 0, \quad \tilde{\nabla} = \left(\frac{\partial}{\partial \xi}, \frac{\partial}{\partial \eta} \right)^T. \quad (14)$$

Next we introduce polar coordinates (r, θ) , where $\xi = r \cos(\theta)$ and $\eta = r \sin(\theta)$ and assume that q is independent of θ :

$$\frac{\partial^2 q}{\partial \tau^2} - \left(\frac{\partial^2 q}{\partial r^2} + \frac{1}{r} \frac{\partial q}{\partial r} \right) = 0. \quad (15)$$

Instead of solving Eq.(15) for one of the primitive variables we will solve it for the velocity potential $\phi(r, t)$, which also satisfies the wave equation. With $u' = \frac{\partial \phi}{\partial x}$ and $v' = \frac{\partial \phi}{\partial y}$ the primitive variables are related to the velocity potential by

$$\frac{\partial \phi}{\partial r} = u'_r, \quad \frac{\partial \phi}{\partial t} = -p', \quad (16)$$

where u'_r is the radial velocity component. The initial conditions can be obtained from these two relations

$$\phi(r, 0) = \int_{\infty}^r u'_r(r) dr = -\frac{\beta}{2\alpha} e^{-\alpha r^2}, \quad (17)$$

$$\frac{\partial \phi}{\partial \tau}(r, 0) = -p'(r, 0) = -e^{-\alpha r^2}. \quad (18)$$

The solution of Eq.(15) for $q = \phi$ with the initial conditions given by Eq.(17) and Eq.(18) can be obtained conveniently by employing the Hankel transform:

$$\phi(r, \tau) = \int_0^{\infty} \lambda J_0(\lambda r) \Phi(\lambda, \tau) d\lambda, \quad (19)$$

$$\Phi(\lambda, \tau) = \int_0^{\infty} r J_0(\lambda r) \phi(r, \tau) dr, \quad (20)$$

where J_0 is the zeroth-order Bessel function of the first kind. Upon applying the Hankel transform the problem reduces to solving

$$\frac{\partial^2 \Phi}{\partial \tau^2} + \lambda^2 \Phi = 0, \quad (21)$$

with

$$\Phi(\lambda, 0) = E(\lambda), \quad \frac{\partial \Phi}{\partial \tau}(\lambda, 0) = F(\lambda), \quad (22)$$

where $E(\lambda)$ and $F(\lambda)$ are given by:

$$\begin{aligned} E(\lambda) &= -\frac{\beta}{2\alpha} \int_0^\infty r J_0(\lambda r) e^{-\alpha r^2} dr, \\ F(\lambda) &= -\int_0^\infty r J_0(\lambda r) e^{-\alpha r^2} dr. \end{aligned} \quad (23)$$

From Gradshteyn and Ryzhik [16] we obtain

$$\int_0^\infty r J_0(\lambda r) e^{-\alpha r^2} dr = \frac{1}{2\alpha} e^{-\frac{\lambda^2}{4\alpha}}. \quad (24)$$

The solution of Eq.(21) can be written as:

$$\Phi(\lambda, \tau) = E(\lambda) \cos(\lambda \tau) + \frac{F(\lambda)}{\lambda} \sin(\lambda \tau). \quad (25)$$

Using Eq.(19) to transform back from λ to r we obtain for the velocity potential:

$$\phi(r, \tau) = -\frac{1}{2\alpha} \left\{ \frac{\beta}{2\alpha} \int_0^\infty \lambda J_0(\lambda r) \cos(\lambda \tau) e^{-\frac{\lambda^2}{4\alpha}} d\lambda + \int_0^\infty J_0(\lambda r) \sin(\lambda \tau) e^{-\frac{\lambda^2}{4\alpha}} d\lambda \right\}. \quad (26)$$

The general solution, as function of r and t , finally becomes:

$$p'(r, t) = \frac{1}{2\alpha} \left\{ \int_0^\infty \lambda J_0(\lambda r) \cos(\lambda t) e^{-\frac{\lambda^2}{4\alpha}} d\lambda - \frac{\beta}{2\alpha} \int_0^\infty \lambda^2 J_0(\lambda r) \sin(\lambda t) e^{-\frac{\lambda^2}{4\alpha}} d\lambda \right\}, \quad (27)$$

$$u'(r, t) = \frac{x - Mt}{2\alpha r} \left\{ \int_0^\infty \lambda J_1(\lambda r) \sin(\lambda t) e^{-\frac{\lambda^2}{4\alpha}} d\lambda + \frac{\beta}{2\alpha} \int_0^\infty \lambda^2 J_1(\lambda r) \cos(\lambda t) e^{-\frac{\lambda^2}{4\alpha}} d\lambda \right\}, \quad (28)$$

$$v'(r, t) = \frac{y}{2\alpha r} \left\{ \int_0^\infty \lambda J_1(\lambda r) \sin(\lambda t) e^{-\frac{\lambda^2}{4\alpha}} d\lambda + \frac{\beta}{2\alpha} \int_0^\infty \lambda^2 J_1(\lambda r) \cos(\lambda t) e^{-\frac{\lambda^2}{4\alpha}} d\lambda \right\}, \quad (29)$$

where

$$r = \sqrt{(x - Mt)^2 + y^2}, \quad (30)$$

and $\rho' = p'$. In the above expressions J_1 is the first-order Bessel function of the first kind.

4.3 Numerical result

For a correct implementation of the initial condition we have to project $\mathbf{U}(x, y, 0)$, given by Eq.(11), onto the basis functions. The integrations which then have to be performed are not straightforward. Alternatively, we will approximate the initial solution by a second-order accurate Taylor-series expansion around the centroid of each element as was also done by Atkins and Shu [4].

In order to perform this 2D calculation with the present 3D method all derivatives in the z -direction are taken equal to zero. Furthermore symmetry-plane boundary conditions are used for the upper and lower boundary in the z -direction. On all the other boundaries of the computational domain characteristic-based non-reflecting boundary conditions are used. Both boundary conditions are described in [7]. We take for the 2D solution the result in the plane $z=0$.

The simulations have been carried out on different tetrahedral meshes. The physical domain,

Ω , is partitioned into N_e identical tetrahedrons obtained by dividing Ω into equally sized cubes, which provides us with a background mesh, and then dividing each cube into 12 identical tetrahedrons. In table 1, specifications of the different meshes are given. The background mesh dimensions are given by N_x , N_y and N_z , while np denotes the number of processors used in the computation. h denotes a characteristic mesh-size, and is given by $h = \frac{1}{N_x}$. All simulations have been carried out with a CFL-number of 0.15.

Case	N_x	N_y	N_z	Tetrahedrons	faces $z = 0$	h	np
II	40	40	2	38,400	3,200	$\frac{1}{40}$	2/4/8/16/32
III	80	80	4	307,200	12,800	$\frac{1}{80}$	*
IV	100	100	5	600,000	20,000 [†]	$\frac{1}{100}$	2/4/8/16/32/64/128
V	120	120	6	1,036,800	28,800	$\frac{1}{120}$	64
VI	160	160	8	2,457,600	51,200	$\frac{1}{160}$	128

* result taken from reference [9]

† 2D result taken in $z = 1$ -plane

Table 1: Mesh specifications and number of processors used for the computations for the different cases

Verification and accuracy

In [9] case IV was already considered with the non-parallel code. The results obtained with the current version of the code shows no differences with the results obtained with this previous version of the code.

Fig.(1) presents the results obtained for p' , along the line $x = 10$ for $t = 20$, for the cases V and VI as well as the analytical solution. The location of the disturbance is accurately resolved in both cases. The magnification of the region $-30 < r < -10$, presented in Fig.(1.b), shows that the result obtained for case VI shows a slightly better comparison with the analytical solution, than the result obtained for case V, as one might have expected.

Fig.(2) presents the results obtained for p' , along the line $x = 20$ for $t = 40$, for the cases IV and VI as well as the analytical solution. The results obtained for case VI show a better agreement with the analytical solution than those of case IV.

In Figures (1) and (2) the graph of the analytical solution is obtained by approximating the integrals in Eq.(27) by means of a composite Simpson's rule. The number of quadrature points is chosen sufficiently high, so that further increasing the number of quadrature points will not be visible in the figures.

For $r = 0$ Eq.(27) can be evaluated exactly, without any numerical approximation. For the pressure perturbation we obtain the analytical solution $p'(0, 20) = -0.016624864$. We denote the numerical approximation of $p'(0, 20)$, computed on a mesh with characteristic size h , by \tilde{p}'_h . In Fig.(3.a) we have plotted $\epsilon = |\tilde{p}'_h - p'(0, 20)|$ vs. h^{-1} on logarithmic scales. The values of the characteristic mesh size h related to the various cases are presented in table (1). The results of case III, V and VI almost lie on a straight line. The result obtained on the coarse mesh of case II only deviates a little from this line. (Note that the result obtained for case IV is not taken into consideration, since the result is not measured in the plane $z = 0$.) The slope of the line gives us the order of the method in the point $(r, t) = (0, 20)$. The slope suggests 5th-order accuracy in the specific point $(r, t) = (0, 20)$. In [17] Hu and Atkins present results of a detailed study of spatially propagating waves in a DG scheme applied to a 1D system of linear hyperbolic equations. They report that the phase error (of the physical mode) decays like h^{2p+2} , where p

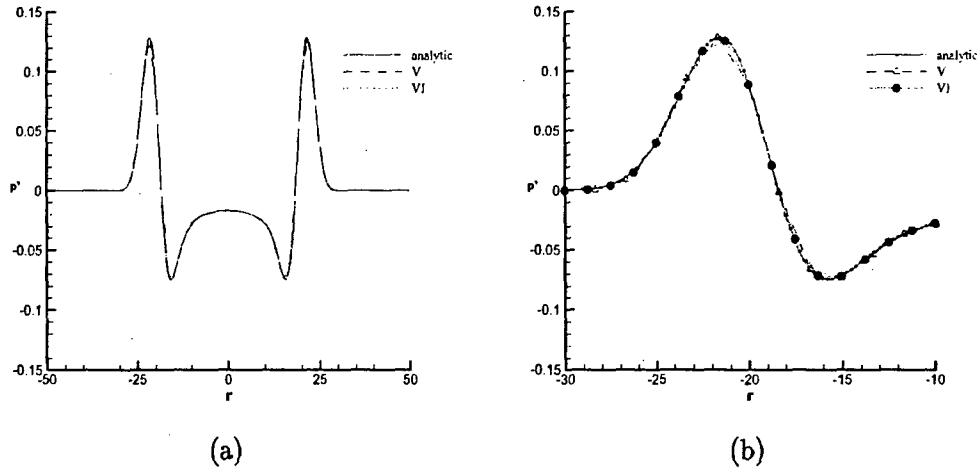


Figure 1: Comparison of numerical results, obtained for case V and VI for $x = 10$ and $t = 20$, with the analytical solution $p'(r, 20)$. b: Magnification of the region $-30 < r < -10$.

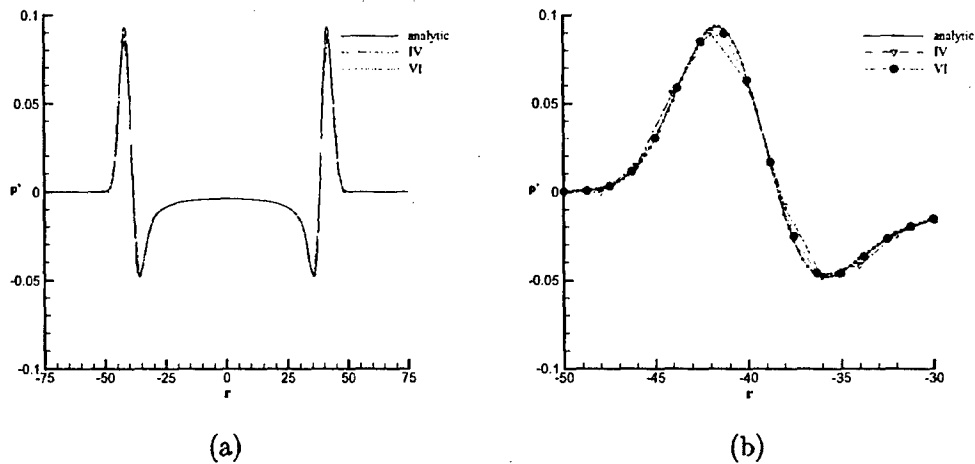


Figure 2: Comparison of numerical results, obtained for case IV and VI for $x = 20$ and $t = 40$, with the analytical solution $p'(r, 40)$. b: Magnification of the region $-50 < r < -30$.

is the degree of the polynomials which are used as basis functions. They also report that the global error measure (for the definition see [17]) reduces at order $2p + 1$. We use basis functions of degree $p = 1$ which would result in a decay of the phase error like h^4 and a decay of the global error measure like h^3 , assuming that the results obtained by Hu and Atkins in 1D would apply to 3D. However, this still does not explain why we observe a decay of the error like h^{2p+3} . Clearly, further research on this topic is necessary.

Assuming that our method is 5th-order accurate in $(r, t) = (0, 20)$, we can apply Richardson extrapolation ([18]) to obtain a prediction of the exact solution. Employing Richardson

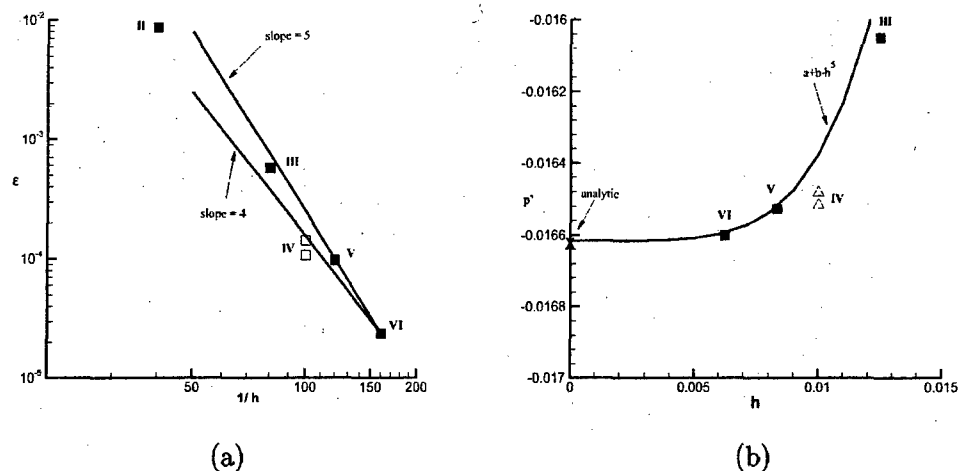


Figure 3: Grid convergence study for the pressure perturbation in $(r, t) = (0, 20)$.

extrapolation we assume that the following holds:

$$\tilde{p}'_h = a + bh^5. \quad (31)$$

Using the numerical results of cases V and VI we can obtain the coefficients a and b . Coefficient a gives the prediction of the exact solution $p'(0, 20)$, we obtain $a = -0.016616442$. The relative error $\left| \frac{a - p'(0, 20)}{p'(0, 20)} \right|$ is approximately 0.05%. Fig.(3.b) shows the polynomial of Eq.(31) together with the numerical results of the different cases.

Speed-up

A performance test has been carried out for case II and IV on TERAS, which is a 1024-CPU platform ([10]) consisting of two 512-CPU SGI Origin 3800 systems. It has a peak performance of 1 TFlops (10^{12} floating point operations per second), it is fitted with 500Mhz R14000 CPU's organized in 256 4-CPU nodes and possesses 1 TByte of total memory. The speed-up is measured in terms of the ratio of the user CPU-times, where the two processor-job serves as reference. From Fig.(4.a) it can be seen that near-linear speed-up is obtained for case IV. Slightly superlinear speed-up is obtained on 4 processors for both case II and IV, which is probably caused by a more efficient cache performance. Fig.(4.a) shows furthermore that by dividing the domain of case II over more than 8 processors, the number of elements assigned to each processor becomes too small and the communication overhead becomes apparent. From Fig.(4.b) we observe that for case IV we have a near-linear speed-up, up to 64 processors. On 128 processors the relative speed-up (relative to $np = 2$) has dropped to 60%.

On 128 processors approximately $8 \cdot 10^9$ floating point operations were performed per second (8 Gflops). For the performance test for case IV, the computation involved 1000 time steps. The computation took less than 8 minutes on 128 processors (elapsed time). TERAS has a peak-performance of 1 Gflops per processor, for case IV the code was observed to operate, on average, at 10% of this peak when up to 8 processors were used. Using increasingly more processors (more than 8) resulted in a gradual drop in performance to approximately 6% of the peak-performance, when 128 processors were used, which is thought to be due to the increased

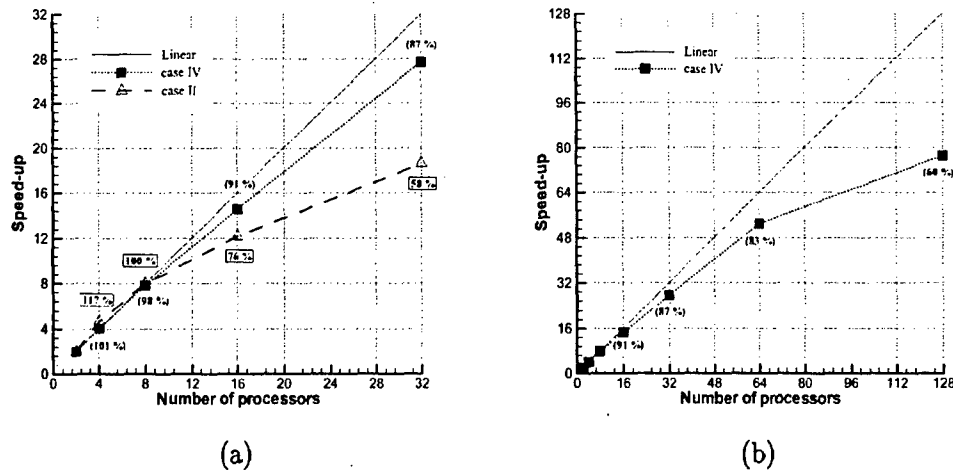


Figure 4: Speed-up measured for case II (100 time steps) and case IV (1000 time steps) on Origin 3800. a: Result for case II and IV for up to 32 processors. b: Result for case IV for up to 128 processors.

communication overhead.

5 Concluding Remarks

The results presented in the present paper are obtained with the computer code DIGS3D, which is based on a numerical algorithm, developed to solve the Linearized Euler equations (LEE) in three dimensions. For the spatial discretization of the LEE the Quadrature-free Discontinuous Galerkin method has been applied, while the time integration is performed by a four-step, low-storage Runge-Kutta algorithm. The algorithm is second-order accurate in both space and time. The main objectives of the work presented in the present paper are (continuation of) the verification of the numerical algorithm and conducting a performance test of the parallelized algorithm on TERAS.

As a verification problem, the convection of a 2D compact acoustic disturbance has been considered on different meshes employing different numbers of processors on TERAS, a 1024-CPU platform consisting of two 512-CPU SGI Origin 3800 systems. The obtained numerical solutions show very good agreement with the analytical solution. A grid convergence study for the pressure perturbation in the centre of the decayed and convected 2D Gaussian pulse at dimensionless time $t = 20$, suggests that the numerical result in that point is 5^{th} -order accurate in the characteristic mesh size. The reason for this unexpected high accuracy, obtained in that specific point with the second order accurate algorithm, is unknown at present and needs further investigation.

The conducted performance test shows, that for a medium-sized mesh (600,000 elements), near-linear speed-up is obtained when up to 64 processors are used. Using 128 processors (for the same problem), shows that a computational speed of approximately 8.10^9 floating point operations per second (8 Gflops) is obtained.

In addition to further verification and validation, future activities will probably include optimization of the algorithm and extension of the algorithm towards higher-order accuracy.

Acknowledgement

The authors like to thank the National Computing Facilities (NCF) foundation for granting computing time on the supercomputer TERAS (Filenumber SG-062).

References

- [1] L.D. Landau and E.M. Lifshitz, *Fluid Mechanics, Course of Theoretical Physics, Volume 6*, Butterworth-Heinemann, reprint 2000.
- [2] C. Johnson and J. Pitkäranta, *An Analysis of the Discontinuous Galerkin method for a Scalar Hyperbolic Equation*, *Mathematics of Computation*, Vol. 46, No 176, pp. 1-26, 1986.
- [3] B. Cockburn, B. Hou and C.W. Shu, *TVB Runge-Kutta Local Projection Discontinuous Galerkin Finite Element Method for Conservation Laws IV: The MultiDimensional Case*, *Mathematics of Computation*, Vol. 54(190), 1990, pp. 545-581.
- [4] H.L. Atkins and C.W. Shu, *Quadrature-Free Implementation of Discontinuous Galerkin method for Hyperbolic Equations*, *AIAA Journal*, Vol. 36, pp. 775-782, 1998.
- [5] H.L. Atkins and D.P. Lockard, *A High-Order Method using Unstructured Grids for the Aeroacoustic Analysis of Realistic Aircraft Configurations*, *AIAA-Paper 99-1945*, 1999, Fifth AIAA/CAES Aeroacoustics Conference, May 10-12.
- [6] H.L. Atkins and C.W. Shu, *Quadrature-Free Implementation of Discontinuous Galerkin method for Hyperbolic Equations*, *AIAA-Paper 96-1683*, 1996.
- [7] H.L. Atkins, *Continued Development of the Discontinuous Galerkin Method for Computational Aeroacoustic Applications*, *AIAA-Paper 97-1581*, 1997.
- [8] C.P.A. Blom, B.T. Verhaar, J.C. van der Heijden and B.I. Soemarwoto, *A Linearized Euler Method Based Prediction of Turbulence Induced Noise using Time-averaged Flow Properties*, *AIAA-Paper 2001-1100*, 39th AIAA Aerospace Sciences Meeting and Exhibit, Reno, Jan. 2001.
- [9] C.P.A. Blom, R. Hagmeijer, A. Biesheuvel and H.W.M. Hoeijmakers, *Three-dimensional Quadrature-free Discontinuous Galerkin Method for Computational Aeroacoustics*, *AIAA-Paper 2001-2198*, 7th AIAA/CEAS Aeroacoustics Conference, Maastricht, May 2001.
- [10] www.sara.nl/Customer/systems/sgi3800.
- [11] A. Baggag, H.L. Atkins, C. Özturan, D. Keyes, *Parallelization of an Object-oriented Unstructured Aeroacoustic Solver*, *NASA/CR-1999-209098*, ICASE Report No. 99-11, February 1999.
- [12] E. Kreyszig, *Introductory Functional Analysis With Applications*, John Wiley & Sons, 1978.

- [13] C. Bailly and D. Juvé, *Numerical Solution of Acoustic Propagation Problems Using Linearized Euler Equations*, AIAA Journal, Vol. 38, Nr. 1, pp. 22-29, Jan. 2000.
- [14] G. Karypis, V. Kumar, *Multilevel k-way partitioning scheme for irregular graphs*, Journal of parallel and distributed computing, Volume 48, No. 1, pp96-129, Jan. 1998.
- [15] H.L. Atkins, *Application of Essentially Nonoscillatory Methods to Aeroacoustic Flow Problems*, Proceedings of ICASE/LaRC Workshop on Benchmark Problems in Computational Aeroacoustics, Edited by J.C. Hardin, J.R. Ristorcelli and C.K.W. Tam, NASA CP-3300, pp. 15-26, 1995.
- [16] I.S. Gradshteyn, I.M. Ryzhik, *Table of Integrals, Series, and Products*, Academic Press, inc. 1980.
- [17] F.Q. Hu and H.L. Atkins, *Eigensolution Analysis of the Discontinuous Galerkin Method with Non-Uniform Grids*, AIAA-Paper 2001-2195, 7th AIAA/CEAS Aeroacoustics Conference, Maastricht, May 2001.
- [18] L. Råde, *Mathematics Handbook*, for Science and Engineering, Fourth Edition, Springer-Verlag Berlin Heidelberg, 1999.

Reference # of Paper: 24

Discusser's Name: Dr. Bastiaan Oskam

Author's Name: Mr. Carl P. A. Blom

Question:

How great is the computational complexity of the DG method in comparison with the DRP scheme on the same finite element mesh? Is it larger than a factor of four?

Answer:

That will depend on the actual wave propagation properties of one method in relation to the other. I can't give a number at this stage because we don't have analytic values for the dispersion and dissipation errors in three dimensions. (I also don't know if these numbers are available for the DRP scheme in three dimensions.) However, on structured meshes the DRP scheme would be expected to be more efficient.

Discusser's Name: Prof. Ir. Joop Slooff

Author's Name: Mr. Carl P. A. Blom

Question:

Apparently you do not know precisely, on an analytical basis, what the order of accuracy is of your scheme. You had to do a numerical mesh convergence experiment to find out. Then, how do you intend to improve the order of accuracy of your method?

Answer:

We did a one dimensional wave propagation analysis that does give us that kind of information. The one dimensional analysis is on a structured mesh. We do not know if we can apply the results obtained in one dimension to three dimensional problems. We also don't know if, and how, it applies to unstructured meshes. Dr Hu [Hu, F. Q., Hussaini, M. Y., and Raestarinera, P., "An analysis of the discontinuous Galerkin method for wave propagation problems," *Journal of Computational Physics*, 141, 1998, pp. 921-946] has presented results of his one-dimensional analysis of wave propagation and showed very promising results. We also did this grid study to enable us to compare with analytical results that might be obtained at a later stage.